

Contribution of the carbohydrate moiety to conformational stability of the carboxypeptidase Y

High pressure study

Mireille Dumoulin¹, Hiroshi Ueno¹, Rikimaru Hayashi¹ and Claude Balny²

¹Division of Applied Life Sciences, Graduate School of Agriculture, Kyoto University, Japan; ²INSERM, Unité 128, IFR 24, CNRS 1919, Montpellier, France

The process of pressure-induced denaturation of carboxypeptidase Y and the role of the carbohydrate moiety in its response to pressure and low temperature were investigated by measuring *in situ* the catalytic activity and, the intrinsic and 8-anilino-1-naphthalene sulfonic acid binding fluorescences.

Pressure-induced denaturation of carboxypeptidase Y is a process involving at least three transitions. Low pressures (below 150 MPa) induced slight conformational changes characterized by a slight decrease in the center of the spectral mass of intrinsic fluorescence, whereas no changes in 8-anilino-1-naphthalene sulfonic acid binding fluorescence were observed and 80% of the catalytic activity remained. Higher pressure (150–500 MPa) induced further conformational changes, characterized by a large decrease in the center of the spectral mass of intrinsic fluorescence, a large increase in the 8-anilino-1-naphthalene sulfonic acid binding fluorescence and the loss of all catalytic activity. Thus, this intermediate exhibited characteristics of molten globule-like state. A further increase, in pressure (above 550 MPa) induced transition from this first molten globule-like state to a second molten globule-like state. This two-stage denaturation process can be explained by assuming the existence of two independent structural domains in the carboxypeptidase molecule.

A similar three-transition process was found for unglycosylated carboxypeptidase Y, but, the first two transitions clearly occurred at lower pressures than those for glycosylated carboxypeptidase Y. These findings indicate that the carbohydrate moiety protects carboxypeptidase Y against pressure-induced denaturation. The origin of the protective effects is discussed based on the known crystallographic structure of CPY.

Keywords: carboxypeptidase Y; fluorescence spectrometry; high pressure; protein denaturation; unglycosylation.

Carboxypeptidase Y (CPY), a 61-kDa vacuolar enzyme from *Saccharomyces cerevisiae* belongs to the family of serine proteases [1]. Its catalytic triad is made of Ser146, Asp338 and His397. This monomeric enzyme, which consists of 421 amino-acid residues and five disulfide bonds, is a glycoprotein [2]. The carbohydrate moiety accounts for about 16% of the molecular mass [3] and consists of four asparagine-linked phosphorylated oligosaccharide chains of roughly equal size [$\text{Man}_{9-18}(\text{GlcNAc})_2(\text{PO}_4^{2-})_{0-2}$] [4–7].

Although much is known about the structure and biosynthesis of the oligosaccharides in CPY, the definitive role of the associated sugar moiety in the structure and function of this enzyme has yet to be established. Studies carried out with carbohydrate-free CPY, obtained by growing yeast in the presence of an inhibitor of N-linked glycosylation or by mutation, showed that the carbohydrate moiety does not affect the processing of the CPY precursor, its accurate vacuolar targeting, or its transport, but the rate of transport of unglycosylated CPY through secretory pathway to the vacuole was reduced [5,8]. Complete removal of carbohydrate by endo

β -N-acetylglucosaminidase H increased the respective rates of SDS-induced inactivation and proteolytic degradation by two and threefold, compared to the rates for glycosylated CPY [9]. However, neither the *in-vivo* nor the *in-vitro* stability and activity of unglycosylated CPY obtained by mutation were significantly different than that of wild-type CPY (WtCPY) [8].

High pressure is increasingly used as a 'reagentless denaturant' to study the protein denaturation [10]. This tool is especially well adapted to the study of cold denaturation of protein because pressure decreases the freezing point of water [11]. Therefore, cold denaturation can be studied without using a cryoprotectant (which may interact with the protein, making interpretation more complicated).

Intrinsic and 8-anilino-1-naphthalene sulfonic acid (ANS)-binding fluorescence spectroscopies are useful techniques to study structural changes during protein denaturation. The intrinsic fluorescence of protein is mainly due to tryptophan and tyrosine residues [12]. The wavelength at maximum fluorescence, thus the center of the spectral mass, depends on the polarity of the environment around these residues, i.e. the center of the spectral mass decreases as the polarity of the environment increases [13]. On the basis of this characteristic, the environment of the tryptophan and tyrosine residues can be monitored experimentally upon protein denaturation. CPY is composed of nine tryptophan and 23 tyrosine residues evenly distributed throughout the entire protein molecule. The intrinsic fluorescence of CPY therefore can be used to trace the overall denaturation. ANS is a fluorescent probe specific for the hydrophobic regions of a protein molecule. It is used to monitor

Correspondence to R. Hayashi, Division of Applied Life Sciences, Graduate School of Agriculture, Kyoto University, Sakyo-ku, Kyoto 606-8502, Japan. Fax: + 81 75 753 6128, Tel.: + 81 75 753 6111.

Abbreviations: ANS, 8-anilino-1-naphthalene sulfonic acid; ATEE, N-acetyl L-tyrosine ethyl ester; CPY, carboxypeptidase Y; Δ glyCPY, unglycosylated CPY; WtCPY, wild-type CPY.

Enzymes: carboxypeptidase Y (EC 3.4.16.1).

(Received 27 January 1999, accepted 10 March 1999)

protein denaturation because its fluorescence is enhanced when it is bound to solvent-exposed hydrophobic areas of proteins [13,14]. Both techniques have been adapted for use in high-pressure studies [10].

Some effects of high pressure on the activity and structure of CPY have been published [15]; but, in those studies the conformational transition could not be fully observed because of technical limitations. Moreover, CPY is very resistant to cold denaturation, i.e. several freezing-thawing cycles at atmospheric pressure do not inactivate this enzyme [1,16]. In our opinion, this unique property of CPY arises from its high oligosaccharide content. For this reason, high pressure appeared to be of special interest for investigating the role of the carbohydrate moiety in the conformational stability and activity of CPY in the low-temperature range. We describe the pressure-induced denaturation process and discuss the possible role of the carbohydrate moiety in the response to high pressure and low temperature based on *in-situ* intrinsic CPY and ANS-binding fluorescence spectroscopy findings and measurements of enzymic activity.

MATERIALS AND METHODS

Enzymes

WtCPY was purified as described previously [1] with modifications [17]. Unglycosylated CPY (Δ glyCPY) was obtained by site-directed mutagenesis. In this mutant enzyme, the asparagine residues of the four Asn-Xaa-Thr glycosylation sites have been replaced by alanine residues. The enzyme was expressed in *S. cerevisiae* and purified by a modification of the procedure used for WtCPY. The main modifications were disruption of the cells by glass beads and the lack of the activation step, not required because Δ glyCPY was already in the active state after cell disruption [18]. Some of the Δ glyCPY we used was prepared by H. Shimizu [18]. Both enzyme preparations were electrophoretically pure. The specific activity of Δ glyCPY was similar to that of WtCPY, therefore it was assumed that complete unglycosylation has no effect on the tertiary structure of the enzyme. Both enzymes were stored in solution in 10 mM potassium phosphate buffer, pH 7, at -20°C and at concentrations of at least $2\text{ mg}\cdot\text{mL}^{-1}$. Under these conditions WtCPY is stable for at least 2 years [1], and Δ glyCPY at least for the duration of this experiment.

Buffer and chemicals

Tris buffer, ANS (lot M6B9346) and *N*-acetyl L-tyrosine ethyl ester (ATEE; lot M3K6958) were obtained from Nacalai Tesque (Kyoto, Japan). Tris/HCl buffer was chosen because its p*K* does not change significantly as a function of pressure [19].

Activity measurement

In-situ effects of pressure on the catalytic activity of CPY were investigated by measuring the apparent second-order rate of ATEE hydrolysis. Absorbance changes at 237 nm were recorded under pressure using a high-pressure optical cell (Teramecs, Kyoto, Japan) set inside a Shimadzu UV-2500 spectrophotometer [20]. The activation volumes (ΔV^\ddagger) were derived from the pressure dependence of the apparent second-order rate constant according to the equation:

$$\Delta V^\ddagger = -RT(\partial \ln k / \partial P)_T = (\Delta G_0 / \partial P)_T \quad (1)$$

where k is the relative apparent second-order rate constant k_{cat}/K_m .

Fluorescence spectroscopy

Both intrinsic and ANS-binding fluorescence measurements were made with a AB2 fluorospectrophotometer (SLM Co.), modified in the INSERM laboratory to measure the fluorescence in the pressure range from 0.1 to 700 MPa through a thermostated high-pressure cell as described previously [21,22]. Each spectrum was the result of three accumulations. Fluorescence intensities were first corrected by subtracting the fluorescence spectra of the buffer (for intrinsic fluorescence) or the free ANS in buffer (for ANS-binding fluorescence) at each pressure. Then, they were corrected for volume contraction under high pressure based on the published compressibility of water and solutions [23].

The excitation wavelength was 280 nm for intrinsic fluorescence measurements, therefore recorded spectra (between 300 and 400 nm) were the sum of the tryptophan and tyrosine contributions. The center of the spectral mass, defined below, was used to quantify the spectra [13,24]:

$$\langle \nu \rangle = \sum \nu_i \times F_i / \sum F_i \quad (2)$$

where ν_i is the wave number and F_i the fluorescence intensity at ν_i .

The excitation wavelength was 350 nm for ANS-binding fluorescence, and emission spectra were recorded between 420 and 600 nm. The fluorescence intensity at the peak wavelength (475 nm) was used to quantify the pressure-induced changes. The ANS concentration was $65\text{ }\mu\text{M}$ in 50 mM Tris/HCl buffer, pH 7, as determined spectrophotometrically at 350 nm using $5000\text{ cm}^{-1}\cdot\text{M}^{-1}$ as the molar absorption coefficient.

Experimental procedures. The enzyme concentration in all the experiments was $0.1\text{ mg}\cdot\text{mL}^{-1}$ ($1.60\text{ }\mu\text{M}$ for WtCPY or $1.95\text{ }\mu\text{M}$ for Δ glyCPY). After each change of temperature or pressure, the system was allowed to equilibrate for 5 min before the spectral recording. When experiments were performed at -5°C , the sample was pressurized to about 100 MPa at 25°C then, the temperature was lowered to -5°C . When experiments were performed at -12.5°C , the sample was pressurized to about 200 MPa at 5°C then the temperature was lowered to -12.5°C . Under these conditions, the sample solution remained in the liquid state. The equilibrium temperature of the solid and liquid of type I ice is lowered as pressure increases up to 200 MPa, pressure at which the freezing temperature of water is about -22°C [11]. The highest pressure that could be applied at a given temperature was derived from the water phase-transition diagram, i.e. about 500 MPa below -5°C [11]. Water condensation and ice formation on the sapphire windows were avoided by flushing them with a fine, dry-nitrogen gas flow.

Determination of thermodynamic parameters. The thermodynamic parameters ΔG_0 and ΔV of the pressure-induced spectral transitions were determined by analyzing the center of the spectral mass (intrinsic fluorescence) or fluorescence intensity at 475 nm (ANS-binding fluorescence). A two-state transition with a constant reaction volume was assumed [25]. If a physical parameter is assumed to take distinct values in these two states, A_1 and A_2 , and an increase of pressure to cause a transition from one to the other state, then the equilibrium constant at a given pressure ($K_{(P)}$) is

$$K_{(P)} = (A_2 - A_{(P)}) / (A_{(P)} - A_1) \quad (3)$$

where $A_{(P)}$ is the intermediate value of the parameter at a given pressure, P .

The pressure dependence of $K_{(P)}$ is related to ΔG at $P = 0.1$ MPa (ΔG_0) and ΔV as follows:

$$-RT \ln(K_{(P)}) = \Delta G_0 + P \times \Delta V \quad (4)$$

Combining Eqns (3) and (4),

$$A_{(P)} = A_2 + (A_1 - A_2) / \{1 + e^{[-(\Delta G_0 + P \times \Delta V) / (RT)]}\} \quad (5)$$

The fit of $A = F(P)$ in Eqn (5) was used to determine the thermodynamic parameters.

The pressure of half transition ($P_{1/2}$) is given by:

$$P_{1/2} = -\Delta G_0 / \Delta V \quad (6)$$

RESULTS

Effect of pressurization at 25 °C on the intrinsic fluorescence of WtCPY and Δ glyCPY

A gradual decrease in the center of the spectral mass of the intrinsic fluorescence spectrum of WtCPY occurred with increasing pressure at 25 °C (Fig. 1A), indicating that the tryptophan and tyrosine residues become more exposed to the solvent (water) due to the pressure-induced unfolding of the WtCPY molecule (pressure limited at 650 MPa). The transition curve did not follow a simple two-state transition, but WtCPY unfolding seemed to occur through a multistep process, of at least three transitions (or four states) although the final state of the third transition was not reached. The first transition was completed at about 130 MPa, the second transition occurred between roughly 200 and 500 MPa and the last transition began at a pressure higher than 540 MPa. After pressure release from the highest pressure tested, changes in the center of the spectral mass of the intrinsic fluorescence were only partially reversible, as shown by the closed circle in Fig. 1A. Based on the clear sigmoidal shape of the second transition, its pseudo-thermodynamic parameters, ΔG_0^{app} and ΔV^{app} , were calculated assuming a two-step transition (the superscript app means the apparent and pseudo-thermodynamic parameters for fundamentally nonequilibrium (irreversible) transition [15]). These parameters were $\Delta G_0^{\text{app}} = 20.6 \text{ kJ} \cdot \text{mol}^{-1}$ and $\Delta V^{\text{app}} = -61 \text{ mL} \cdot \text{mol}^{-1}$. The pressure of half transition was 334 MPa.

Effects of pressure increases at 25 °C on the intrinsic fluorescence of Δ glyCPY were similar to those for WtCPY (Fig. 1B); the unfolding of Δ glyCPY also proceeded via at least three transitions. This suggests that the carbohydrate moiety does not affect the global unfolding pathway of CPY. After pressure release from the highest pressure applied, the changes observed were only partly reversible, as shown by the closed circle. The main difference between WtCPY and Δ glyCPY is that the first and second transitions clearly occurred at lower

pressures for Δ glyCPY, suggesting that its conformation is more easily perturbed by the pressure. Indeed, the pressure of the half-second transition was $P_{1/2} = 282$ MPa; 52 MPa lower than that of WtCPY. The pseudo-thermodynamic parameters were $\Delta G_0^{\text{app}} = 22.9 \text{ kJ} \cdot \text{mol}^{-1}$ and $\Delta V^{\text{app}} = -80 \text{ mL} \cdot \text{mol}^{-1}$. The

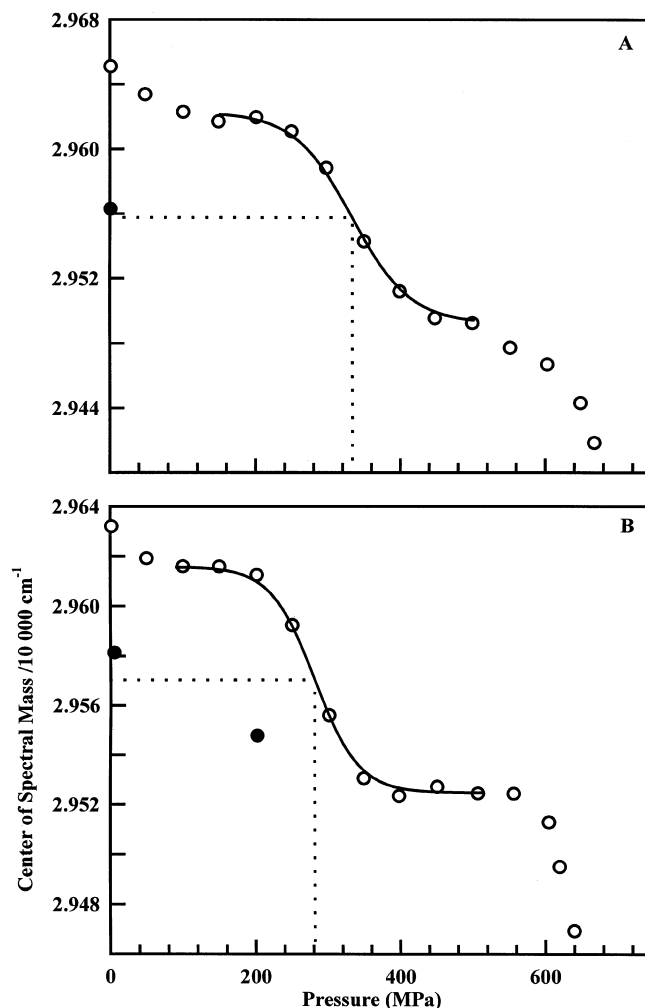


Fig. 1. *In-situ* pressure-induced changes in the center of the spectral mass (intrinsic fluorescence) of WtCPY (A) and Δ glyCPY (B). Pressure increase (○); pressure release from the highest pressure (●). Temperature, 25 °C; [Enzyme] = 0.1 mg·mL⁻¹ in 50 mM Tris/HCl buffer, pH 7. Excitation wavelength, 280 nm. Curves fitted to the second transition were drawn for WtCPY (A) using, $\Delta G_0^{\text{app}} = 20.6 \text{ kJ} \cdot \text{mol}^{-1}$, $\Delta V^{\text{app}} = -61 \text{ mL} \cdot \text{mol}^{-1}$; and for Δ glyCPY (B), $\Delta G_0^{\text{app}} = 22.9 \text{ kJ} \cdot \text{mol}^{-1}$, $\Delta V^{\text{app}} = -80 \text{ mL} \cdot \text{mol}^{-1}$. Dotted lines show the half of the second transition.

Table 1. Apparent pseudo-thermodynamic parameters of pressure-induced transition between 150 and 500 MPa for WtCPY and Δ glyCPY measured at different temperatures. Standard errors are approximately $\pm 5\%$. ND, not determined because transition was not complete (see text). NM, not measured.

Temperature (°C)	WtCPY			Δ glyCPY		
	ΔG_0^{app} (kJ·mol ⁻¹)	ΔV^{app} (mL·mol ⁻¹)	$P_{1/2}$ (MPa)	ΔG_0^{app} (kJ·mol ⁻¹)	ΔV^{app} (mL·mol ⁻¹)	$P_{1/2}$ (MPa)
25	20.6 ^a	-61 ^a	334 ^a	22.9 ^a	-80 ^a	282 ^a
	16.5 ^b	-47 ^b	344 ^b	18.7 ^b	-59 ^b	309 ^b
-5	15.0 ^a	-64 ^a	229 ^a	24.8 ^a	-129 ^a	190 ^a
	19.6 ^b	-93 ^b	208 ^b	19.0 ^b	-102 ^b	183 ^b
-12.5	ND	ND	165 ^a	ND	ND	135 ^a
	NM	NM	NM	NM	NM	NM

^a Value determined from tryptophan intrinsic fluorescence spectroscopy; ^b value determined from ANS-binding fluorescence spectroscopy.

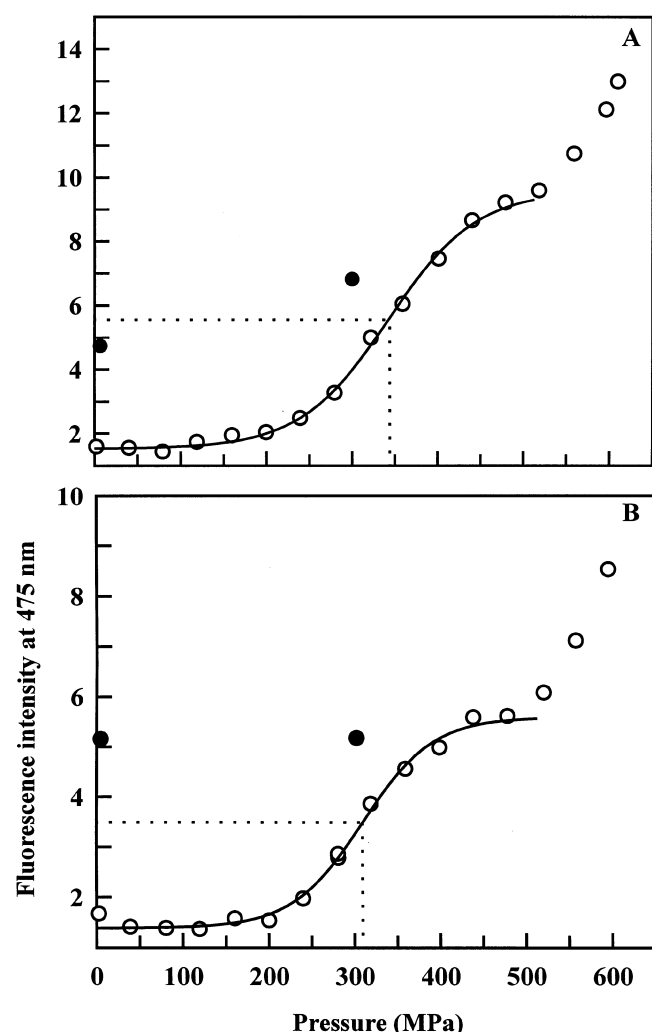


Fig. 2. *In-situ* pressure-induced changes in the ANS-CPY binding fluorescence of WtCPY (A) and ΔglyCPY (B). Pressure increase (○); pressure release from the highest pressure (●). Temperature, 25 °C; [Enzyme] = 0.1 mg·mL⁻¹ in 50 mM Tris/HCl buffer pH 7; [ANS] = 65 μM in 50 mM Tris/HCl buffer, pH 7. Excitation wavelength, 350 nm. Curves fitted to the second transition were drawn for WtCPY (A) using, $\Delta G_0^{\text{app}} = 16.5 \text{ kJ}\cdot\text{mol}^{-1}$, $\Delta V^{\text{app}} = -47 \text{ mL}\cdot\text{mol}^{-1}$; and for ΔglyCPY (B), $\Delta G_0^{\text{app}} = 18.7 \text{ kJ}\cdot\text{mol}^{-1}$, $\Delta V^{\text{app}} = -59 \text{ mL}\cdot\text{mol}^{-1}$. Dotted lines show the half of the second transition.

lower $P_{1/2}$ -value than WtCPY was due to a larger negative ΔV^{app} (Table 1).

Effect of pressurization at 25 °C on the ANS-binding fluorescence of WtCPY and ΔglyCPY

ANS-binding fluorescence was also used to study conformational changes induced by pressure. Figure 2A shows the

Table 2. Activation volume ΔV^\ddagger determined from pressure dependence of the apparent second-order rate of ATEE hydrolysis by WtCPY and ΔglyCPY measured at 25 °C. Standard errors are approximately 5%.

Pressure (MPa)	ΔV^\ddagger (mL·mol ⁻¹)	
	WtCPY	ΔglyCPY
< 200	3.3	4.5
> 200	21.8	34.3

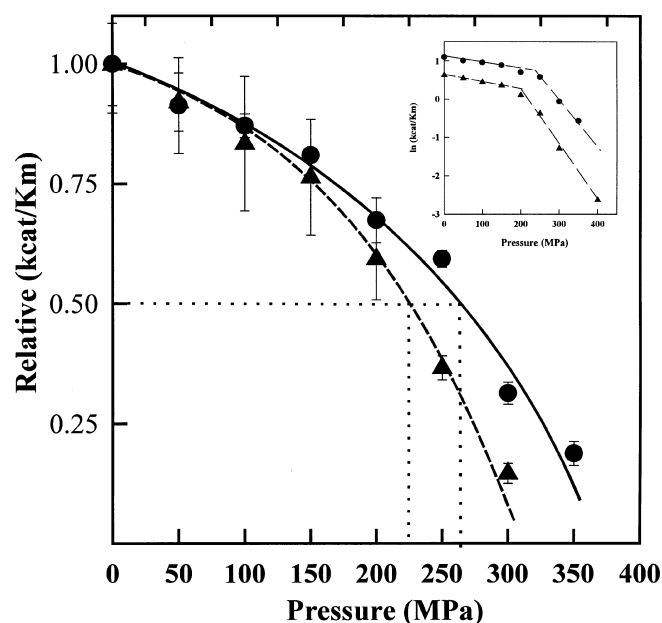


Fig. 3. *In-situ* pressure-induced changes in the apparent second-order rate constant of ATEE hydrolysis. (●), WtCPY; (▲) ΔglyCPY. Temperature, 25 °C; [ATEE] = 0.2 mM in 50 mM Tris/HCl buffer, pH 7; [Enzyme] = 20–60 nM (depending on the activity). Apparent rate constants are relative to that at 0.1 MPa and 25 °C. A new enzyme/substrate solution was used for each pressure. Measurements were repeated under each condition at least twice. Error bars are smaller than the symbols when not visible. Dotted lines show the pressure causing 50% inactivation. Inset, $\ln(k_{\text{cat}}/K_m)$ vs. pressure.

fluorescence intensity at 475 nm (wavelength peak of bound ANS) of ANS-WtCPY as a function of pressure. At 0.1 MPa, the fluorescence intensity was relatively low, indicating that ANS has only very low affinity for native WtCPY. As pressure increased, ANS-binding fluorescence was progressively enhanced (open circle) indicating that ANS binds progressively to WtCPY as the pressure increases, in other words the

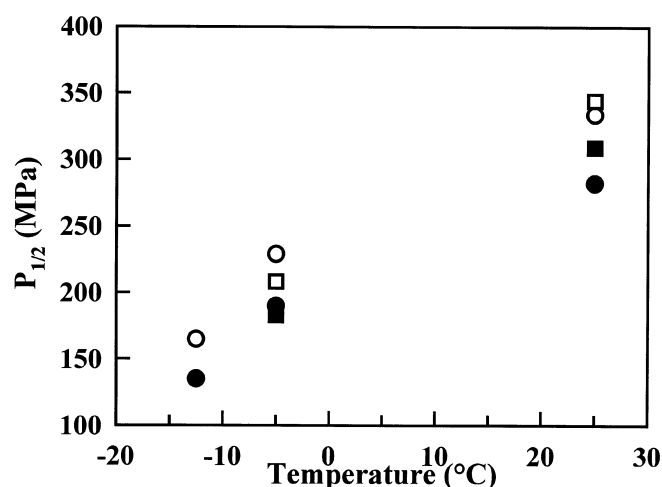


Fig. 4. Temperature dependence of the pressure of half the transition ($P_{1/2}$) that occurred between 150 and 500 MPa. [Enzyme] = 0.1 mg·mL⁻¹ in 50 mM Tris/HCl buffer, pH 7. From intrinsic fluorescence: (○), WtCPY; (●), ΔglyCPY. From ANS-binding fluorescence: (□), WtCPY; (■), ΔglyCPY.

hydrophobic core of WtCPY becomes more exposed to solvent due to pressure-induced unfolding. Upon pressure release, the fluorescence intensity at 475 nm decreased but did not return to the initial value (closed circle). The transition curve of ANS-binding fluorescence did not follow a single two-state transition, but occurred through two transitions (or three states). This differs from the three-transition process found with intrinsic fluorescence spectroscopy (Fig. 1A). Indeed, at pressures lower than 200 MPa, where the first transition occurred with intrinsic fluorescence, there was almost no ANS-binding fluorescence increase. The first ANS-binding fluorescence transition occurred roughly between 200 and 540 MPa. The pseudo-thermodynamic parameters for this transition were ΔG_0^{app} 16.5 kJ·mol⁻¹ and ΔV^{app} = -47 mL·mol⁻¹. The pressure of half transition was 344 MPa. The good agreement of this latter value with that of the second transition determined from the intrinsic fluorescence of WtCPY (334 MPa) suggests that they correspond to the same conformational transition. The second transition of ANS-binding fluorescence started at a pressure higher than 540 MPa and no saturation was observed even at the highest pressure applied (630 MPa).

The pressure increase induced similar changes in ANS- Δ glyCPY fluorescence (Fig. 2B), but the first transition occurred at a pressure lower than that for WtCPY ($P_{1/2}$ was 309 and 344 MPa, respectively). After pressure release, the changes in ANS-binding fluorescence were also only partly reversible (Fig. 2B, closed circle). The pseudo-thermodynamic parameters for this transition were ΔG_0^{app} = 18.7 kJ·mol⁻¹ and ΔV^{app} = -59 mL·mol⁻¹.

Effects of pressurization at 25 °C on catalytic activity of WtCPY and Δ glyCPY

Figure 3 shows the pressure dependence (compared to that at 0.1 MPa) of the relative apparent second-order rate of the hydrolysis of ATEE for both WtCPY and Δ glyCPY at 25 °C and pH 7. A fresh enzyme/substrate solution was used for each pressure treatment. The substrate concentration was kept at 0.2 mM (roughly < 10% of K_m) in order to access the apparent second order rate. The activation volumes (ΔV^\ddagger) were calculated from Eqn (1). As shown in Fig. 3 inside, the plot of $\ln(k_{\text{cat}}/K_m)$ vs. pressure was linear but biphasic. This behavior may be related to the multistep process observed with intrinsic fluorescence spectroscopy. The pressure producing a 50% decrease in the activity was 260 MPa for WtCPY and 230 MPa for Δ glyCPY. To calculate ΔV^\ddagger , two pressure ranges were considered: from 0.1 to 200 MPa and pressures above 200 MPa. Table 2 gives the values obtained. The extent of inactivation was limited for WtCPY and Δ glyCPY at pressures lower than 200 MPa, ΔV^\ddagger was 3.3 and 4.5 mL·mol⁻¹, respectively, for WtCPY and Δ glyCPY. At higher pressures, both enzymes were more extensively inactivated. In the pressure domain above 200 MPa, ΔV^\ddagger was 21.8 and 34.3 mL·mol⁻¹, respectively, for WtCPY and Δ glyCPY. Under 400 MPa, the maximum pressure for absorption measurement in our laboratory, the remaining activity of Δ glyCPY was 3.3%. As 400 MPa coincides only just to the end of the second transition (slight changes of ANS-binding fluorescence occurred up to 450 MPa), it is likely that a small amount of nondenatured protein remains under this pressure. Thus, the remaining activity is likely to be associated with the nondenatured protein, whereas the denatured protein is fully inactive. The same conclusion can be inferred for WtCPY.

Effects of temperature on pressure-induced conformational changes

The effects of pressure at subzero temperatures (-5 and -12.5 °C) on the conformation of WtCPY and Δ glyCPY were investigated. To keep the sample in the liquid state, the pressure was first set near the target value then, the temperature was lowered to the desired value (see Materials and methods).

Because of the technical restraints described above, the transition that occurred at about 100 MPa at 25 °C in the intrinsic fluorescence studies was not observable in experiments at subzero temperatures. At -5 °C, the second transition was completed (both initial and final plateaus were observed) and the pseudo-thermodynamic parameters could be calculated, but the final point of the third transition could not be reached. At -12.5 °C, the first point was determined under 200 MPa and was located on the exponential transition. In other words, roughly half the second transition was reached. Therefore, $P_{1/2}$ could only be estimated. The third transition was not completed. Studies of ANS-binding fluorescence were also performed at -5 °C.

Table 1 gives all the pseudo-thermodynamic parameters determined for the transition that occurs between 150 and 500 MPa. The $P_{1/2}$ -values found for the intrinsic and ANS-binding fluorescence at a given temperature are quite similar (Table 1). For both enzymes, in both intrinsic and ANS-binding fluorescence studies, there is the tendency for $P_{1/2}$ to decrease with a decrease in temperature (Fig. 4). This is consistent with the elliptical shape for enzyme inactivation and denaturation reported by others [26,27]. In general, the decrease in $P_{1/2}$ with the decrease in temperature was due to marked drop in ΔV^{app} (Table 1). Figure 4 also indicates that $P_{1/2}$ for Δ glyCPY is about 45 MPa lower than that for WtCPY at any given temperature of pressurization. This difference is mainly due to a larger negative ΔV^{app} for Δ glyCPY than for WtCPY (Table 1), whereas ΔG_0^{app} seems to be less affected.

DISCUSSION

Pressure-induced denaturation process of CPY

Results of *in-situ* intrinsic and ANS-binding fluorescence and those of enzymic inactivation under pressure showed that pressure-induced denaturation of CPY at 25 °C underwent the same global pathway whether or not the enzyme was glycosylated. A process of at least three transitions is inferred.

Relatively low pressures (below 150 MPa) induced conformational changes as shown by the decrease in the center of the spectral mass of the intrinsic fluorescence spectra (Fig. 1). These conformational changes are probably small as the amplitude of the changes in the center of the spectral mass is small and the hydrophobic core of the protein is not affected (no increase in ANS-binding fluorescence, Fig. 2). Moreover, in that pressure range, almost 80% of the catalytic activity of both enzymes remained (Fig. 3). Because the structural changes in this pressure region are small, this slight decrease in activity might be due to direct pressure effects on catalytic phenomena.

Higher pressures, between 150 and 500 MPa, induced greater change in the intrinsic fluorescence spectra with a concomitant increase in the exposure of the CPY hydrophobic core to the solvent (Figs 1 and 2). In that pressure range, denatured enzymes lost all their activity. Therefore, conformational changes observed in this pressure range probably correspond to alterations of the active-site structure. Moreover, it is likely

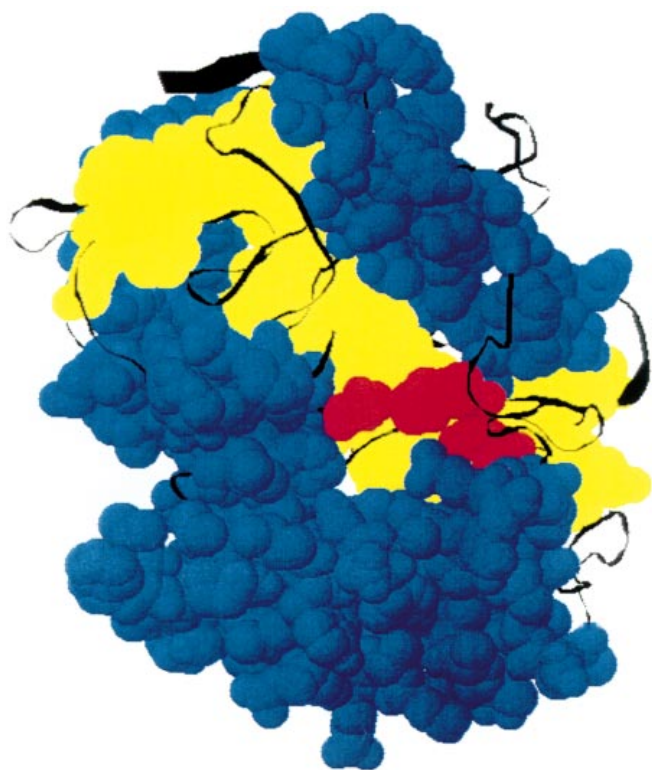
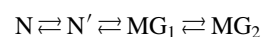


Fig. 5. Space-filling model of CPY showing the two substructural domains of CPY molecule. Based on X-ray crystallographic data of Endrizzi *et al.* [4]. Helixes are shown in blue, β -sheets in yellow and catalytic triad in red.

that this pressure-induced intermediate is a molten globule-like state because the loss of activity and capacity to bind ANS are two characteristic properties of a molten globule structure. Previous reports also support the evidence of a molten globule-like state [15].

The high pressures of up to 650 MPa applied showed an additional transition in the fluorescence spectra at pressures higher than ≈ 540 MPa (Figs 1 and 2). The question of whether this new transition corresponds to conversion from the molten globule-like state to the completely denatured state or to a second molten globule-like state is addressed. Because this transition is characterized by a marked enhancement of ANS-binding fluorescence, it is likely that this transition leads to the formation of a second molten globule-like state. Thus, at least two intermediates exhibiting molten globule-like structure are sequentially obtained upon pressure-induced denaturation. Such 'multiple molten globule-like state transitions' processes have also been reported for other proteins [28,29], however, it differs completely from results reported for the tetrameric carboxypeptidase A and the tetrameric carboxypeptidase from *Sulfolobus solfataricus* [21,30].

The following plausible denaturation pathway accounting for the data presented above can be given:



where N is the native state; N', the native-like state; MG₁, the first molten globule-like state; and MG₂, the second molten globule-like state. After the pressure release from highest pressure applied, the conformational changes were only partly reversible. However, the results presented here do not allow one to determine which stage is responsible for irreversibility. Indeed, the reversibility was checked after pressure release from a pressure at which the third transition has already started. Besides, irreversibility may be due to the fact that a pro-region in the pre-matured protein is required for the correct refolding of CPY [31,32], although a possible aggregation of the (partially) unfolded molecule can not be ruled out.

The state N' has a conformation similar to that of the native state: the environment of the aromatic residues is only slightly more polar and the hydrophobic core is not affected. Thus, N' can be the equilibrium intermediate counterpart of the most structured folding (kinetic) intermediate.

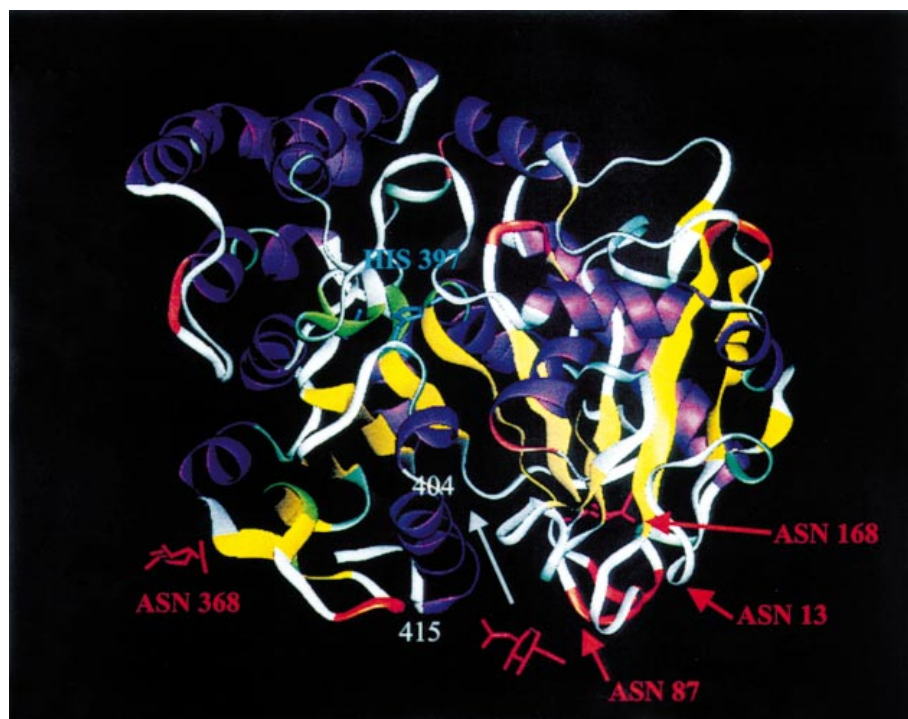


Fig. 6. Ribbon diagram of CPY. Based on X-ray crystallographic data of Endrizzi *et al.* [4] and viewed on a SGI Indigo2-EX computer. Residues of active site are colored blue, and carbohydrate chains red. α -Helixes are shown in purple and β -sheets in yellow. Carbohydrate chain attached to Asn13 is not available from the data base.

N' is further successively unfolded into MG₁ and MG₂ as pressure increases. Two models can be proposed to explain a two-step transition process.

(a) Each of the transition embraces the whole molecule in two successive partial melting processes. Or in other words, the molten globule-like properties in both MG₁ and MG₂ encompass the entire polypeptide chain: the whole molecule is melted into a first molten globule, which is then melted into a second molten globule state. Such a pathway has been suggested for other proteins [29]. In such cases, the second molten globule state is less compact than the first molten globule state; it still has a partial secondary structure and binds ANS but less than the first molten globule state. Thus, our results do not support this model because MG₂ binds more ANS than MG₁.

(b) Alternately, the two-step pathway can be explained by a sequential unfolding of at least two structural domains. In other words, the protein molecule is assumed to be composed of at least two domains and each of which unfolds independently. According to this model, MG₁ corresponds to the melting of one domain into a molten globule-like state, whereas the second domain preserves its native conformation. The MG₂ corresponds to the melting of the second domain into a molten globule-like state.

Structural inspection of the tertiary structure of CPY gives evidences consistent with this latter model. Figure 5 shows that the secondary elements of CPY form two clear domains: the central core is formed by β -sheets, whereas helices are on the external part of the molecule. Thus, it is likely that these two structural domains of CPY undergo conformational changes nonsimultaneously, showing that they are independent and differ in stability against high pressure-induced denaturation. The next question is: which domain unfolds first upon pressurization? We showed that the transition leading to MG₁ is concomitant with the loss of activity, thus with the alteration of the active site. However, because the catalytic triad is located at the interface of the two domains, results presented here do not yet allow one to definitely answer the above question.

Role of the carbohydrate moiety of CPY, in pressure-induced denaturation

In the absence of the carbohydrate moiety, the pressure of the half transition of the center of the spectral mass was lowered by about 50 MPa at 25 °C (Table 1). Although the difference is small, it was consistently observed at all the temperatures investigated. Results of ANS-binding fluorescence (Table 1) and enzyme inactivation (Fig. 3, Table 2) closely parallel the finding of intrinsic tryptophan fluorescence and provide additional evidence that glycosylation enhances the conformational stability of the active site against pressure. Whereas a distinct difference, in pressure stability was found, our results do not explain the molecular basis by which carbohydrate affects CPY properties.

CD spectra in the far UV indicated that the secondary structure of Δ glyCPY is similar to that of WtCPY [18]. Moreover, unglycosylation does not affect the tertiary structure of CPY (Δ glyCPY has the same specific activity as WtCPY), this is consistent with the fact that the four glycosylation sites are located on the protein surface, and none is close to the active site of the enzyme [4] (Fig. 6). However, WtCPY was less easily perturbed than Δ glyCPY. Consequently, although glycosylation has negligible effects, if any, on CPY overall secondary and tertiary structure, it induces local rearrangements, which enhance the stability of the enzyme. The view of local

reorganization in the vicinity of glycosylation sites is supported by results reported for other glycoproteins [33,34].

The lower $P_{1/2}$ may be due to a lower ΔG_0^{app} and/or larger ΔV^{app} (see Eqn 6). From the data in Table 1, the ΔG_0^{app} for Δ glyCPY is generally slightly larger than that for WtCPY. The lower $P_{1/2}$ -values observed for Δ glyCPY were therefore due to a markedly larger negative ΔV^{app} , and only the effects of the carbohydrate moiety on the changes in volumes are discussed below, neglecting the changes in ΔG_0^{app} . Changes in the reaction volume on pressurization are commonly explained in terms of (a) intrinsic contribution and (b) solvent contribution [10].

(a) *Effects of the carbohydrate moiety on cavities (intrinsic contribution).* The intrinsic contribution is mainly due to reduction of the internal cavities associated with the imperfect packing of amino-acid residues [10]. Because all the carbohydrate chains are located on the surface of the protein molecule, we believe that their removal does not form additional internal cavities, which would have, in turn, led to a larger volume decrease under pressure. Although we cannot rule out the possibility that protective effects described below indirectly influence the effect of pressure on the compressibility of normal CPY cavities, we assume that protection arises mainly from different hydration properties (solvent contribution) due to local rearrangements in the vicinity of the glycosylation chains.

(b) *Effects of carbohydrate moieties on the protein hydration (solvent contribution).* Local rearrangements by which a carbohydrate moiety protects CPY may consist in the formation of noncovalent interactions between the carbohydrate moiety and the peptide backbone. These interactions will decrease the protein conformational mobility and thus stabilize the protein. NMR studies performed on a variety of glycoproteins have shown that the carbohydrate moiety forms not only hydrogen bonds but also hydrophobic interactions and van der Waals contacts with the protein moiety [33,35,36]. For example, in the crystal structure of glucose oxidase it was shown that the N-linked mannose residue forms strong hydrogen bonds with the backbone nitrogen and carbonyl oxygen of glutamic acid [35]. Rearrangements in the fucosylated proteinase inhibitor probably originate from hydrophobic interaction between the methyl group of Thr16 and that of fucose, as well as from hydrophobic and hydrogen-bond interactions involving Arg18 and the fucosylated Thr9 [33]. A diagram of CPY (Fig. 6) shows that Asn13 is located in a loop, Asn87 at the last residue of an α -helix, Asn168 between an α -helix and one residue before a β -sheet, and Asn368 in the middle of a β -sheet. Carbohydrate chains at position 87, 168, and 368 may stabilize, via noncovalent interactions, the secondary structure they are close to. It is important to emphasize that the helix containing Asn87 is located in front of α -helix 404–415, which is connected both to the C-terminal residue and His397, a constitutive amino acid of the catalytic site (Fig. 6). The carbohydrate attached to Asn87 therefore may link these two helices via noncovalent interactions thereby stabilizing the active site region. Because hydrogen bonds are stable under pressure, whereas hydrophobic interactions are disrupted [10,37], our results suggest that carbohydrate moiety may enhance CPY stability mainly via the formation of hydrogen bonds between the protein and carbohydrate moieties.

Protection by carbohydrate may also be due to steric hindrance between the sugar and the protein molecule, resulting in reduced solvent accessibility or differential ordering of the water structure around the glycosylation site [38–40]. Again,

this effect might be of special importance around the carbohydrate chain linked to Asn87. This chain may form a bridge, via hydrogen bonding, between the helix containing Asn87 and the facing α -helix 404–415. Such linkage would result in reduced accessibility of water into the crevice (which is shown by the gray arrow in Fig. 6) that separates these two domains of the CPY molecule. The fact that hydration changes associated with the diffusion of water into cavities contribute to the volume decrease observed during protein unfolding [10,37] supports our assumption.

Finally, we stress the efficacy of using this high-pressure technique to show the contribution of the carbohydrate moiety to CPY conformational stability, which is not possible using the usual denaturation studies [18].

ACKNOWLEDGMENTS

We thank N. Bec, Dr J. Connelly, J. L. Saldana and C. Valentin (INSERM U 128) for their expert technical assistance, and are grateful to Prof. A. H. Hooper (University of Minnesota) and Dr E. Mombelli (INSERM U 128) for their critical reading of the manuscript. This work has been partly supported by a grant from the Institut National de la Santé et de la Recherche Médicale and the Japan Society for the Promotion of Science, and a Grant-Aid for Scientific Research from the Ministry of Education, Science, Culture and Sports, Japan.

REFERENCES

- Hayashi, R. (1976) Carboxypeptidase Y. *Methods Enzymol.* **45**, 568–587.
- Hata, T., Hayashi, R. & Doi, E. (1967) Purification of yeast proteinases. Part III. Isolation and physicochemical properties of yeast proteinase A and C. *Agric. Biol. Chem.* **31**, 357–367.
- Aribara, S., Hayashi, R. & Hata, T. (1971) Physical and chemical properties of yeast proteinase C. *Agric. Biol. Chem.* **35**, 658–666.
- Endrizzi, J.A., Breddam, K. & Remington, S.J. (1994) 2.8-Å Structure of yeast serine carboxypeptidase. *Biochemistry* **33**, 11106–11120.
- Hasilik, A. & Tanner, W. (1978) Biosynthesis of the vacuolar yeast glycoprotein carboxypeptidase Y. Conversion of precursor into the enzyme. *Eur. J. Biochem.* **85**, 599–608.
- Hashimoto, C., Cohen, R.E., Zhang, W.-J. & Ballou, C.E. (1981) Carbohydrate chains on yeast carboxypeptidase Y are phosphorylated. *Proc. Natl Acad. Sci. USA* **78**, 2244–2248.
- Trimble, R.B., Maley, F. & Chu, F.K. (1983) Glycoprotein biosynthesis in yeast. *J. Biol. Chem.* **258**, 2562–2567.
- Winther, J.R., Stevens, T.H. & Kielland-Brandt, M.C. (1991) Yeast carboxypeptidase Y requires glycosylation for efficient intracellular transport, but not for vacuolar sorting, *in vivo* stability, or activity. *Eur. J. Biochem.* **197**, 681–689.
- Chu, F.K. & Maley, F. (1982) Stabilization of the structure and activity of yeast carboxypeptidase Y by its high-mannose oligosaccharide chains. *Arch. Biochem. Biophys.* **214**, 134–139.
- Mozhaev, V.V., Heremans, K., Frank, J., Masson, P. & Balny, C. (1996) High pressure effects on protein structure and function. *Proteins* **24**, 81–91.
- Bridgman, P.W. (1912) Water in the liquid and fine solid forms under pressure. *Proc. Am. Acad. Arts Sci.* **47**, 441–558.
- Hamaguchi, K. (1992) Physico-chemical properties of amino acid side chains. In *The Protein Molecule. Conformation, Stability and Folding* (Hamaguchi, K., ed), pp. 1–19. Japan Scientific Society Press, Tokyo.
- Ruan, K., Lange, R., Bec, N. & Balny, C. (1997) A stable partly denatured state of trypsin induced by high hydrostatic pressure. *Biochem. Biophys. Res. Commun.* **239**, 150–154.
- Cléry, C., Renault, F. & Masson, P. (1995) Pressure-induced molten globule state of cholinesterase. *FEBS Lett.* **370**, 212–214.
- Kunugi, S., Yanagi, Y., Kitayaki, M., Tanaka, N. & Uehara-Kunugi, Y. (1997) Effects of high-pressure on the activity and spectroscopic properties of carboxypeptidase Y. *Bull. Chem. Soc. Jpn.* **70**, 1459–1463.
- Hayashi, R., Kinsho, T. & Ueno, H. (1998) Combined application of sub-zero temperature and high pressure on biological materials. In *High Pressure Food Science, Bioscience and Chemistry* (Isaacs, N.S., ed.), pp. 166–174. Royal Society of Chemistry, England.
- Jung, G., Ueno, H., Hayashi, R. & Liao, T.-H. (1995) Identification of the catalytic histidine residue participating in the charge-relay system of carboxypeptidase Y. *Protein Sci.* **4**, 2433–2435.
- Shimizu, H., Ueno, H. & Hayashi, R. (1999) Role of carbohydrate moiety in carboxypeptidase Y: structural study of mutant enzyme lacking carbohydrate moiety. *Biosci. Biotechnol. Biochem.* in press.
- Neumann, R.C., Kauzmann, W. & Zipp, A. (1973) Pressure dependence of weak acid ionization in aqueous buffers. *J. Phys. Chem.* **77**, 2687–2691.
- Morishita, M., Tanaka, T. & Kawai, S. (1997) High pressure optical cell and its pump for spectrophotometer. In *High Pressure Bioscience and Technology* (Suzuki, A. & Hayashi, R., eds), pp. 187–194. San-ei Shuppan Co., Kyoto, Japan (in Japanese).
- Bec, N., Villa, A., Tortora, P., Mozhaev, V.V., Balny, C. & Lange, R. (1996) Enhanced stability of carboxypeptidase from *Sulfolobus solfataricus* at high pressure. *Biotechnol. Lett.* **18**, 482–488.
- Lange, R., Frank, J., Saldana, J.-L. & Balny, C. (1996) Fourth derivative UV-spectroscopy of proteins under high pressure. I. Factors affecting the fourth derivative spectrum of the aromatic amino acids. *Eur. Biophys. J.* **24**, 277–283.
- Gibson, R.E. & Loeffler, O.H. (1941) Pressure–volume–temperature relations in solutions. V. The energy–volume coefficients of the carbon tetrachloride, water and ethylene glycol. *J. Am. Chem. Soc.* **63**, 898–906.
- Silva, J.L., Miles, E.V. & Weber, G. (1986) Pressure dissociation and conformational drift of the β -dimer of tryptophan synthase. *Biochemistry* **25**, 5780–5786.
- Balny, C., Travers, F., Barman, T. & Douzou, P. (1987) Thermodynamics of the two-step formation of horseradish peroxidase compound I. *Eur. Biophys. J.* **14**, 375–383.
- Hawley, S.A. (1971) Reversible pressure-temperature denaturation of chymotrypsinogen. *Biochemistry* **10**, 2436–2442.
- Taniguchi, Y. & Suzuki, K. (1983) Pressure inactivation of α -chymotrypsin. *J. Phys. Chem.* **87**, 5185–5193.
- Masson, P. & Cléry, C. (1996) Pressure-induced molten globule states of proteins. In *High Pressure Bioscience and Biotechnology* (Hayashi, R. & Balny, C., eds), pp. 114–126. Elsevier Science B.V., the Netherlands.
- Ptitsyn, O.B. (1995) Molten globule and protein folding. *Adv. Prot. Chem.* **47**, 83–229.
- Mombelli, E., Bec, N., Tortora, P., Balny, C. & Lange, R. (1996) Pressure and temperature control of a thermophilic carboxypeptidase from *Sulfolobus solfataricus*. *Food Biotech.* **10**, 131–142.
- Winther, J.R. & Sørensen, P. (1991) Propeptide of carboxypeptidase Y provides a chaperone-like function as well as inhibition of the enzyme activity. *Proc. Natl Acad. Sci. USA* **88**, 9330–9334.
- Sørensen, P., Winther, J.R., Kaarsholm, N.C. & Poulsen, F.M. (1993) The pro region required for folding of carboxypeptidase Y is a partially folded domain with little regular structural core. *Biochemistry* **32**, 12160–12166.
- Mer, G., Hietter, H. & Lefèvre, J.-F. (1996) Stabilization of protein by glycosylation examined by NMR analysis of a fucosylated proteinase inhibitor. *Nat. Struct. Biol.* **3**, 45–53.
- Wang, F.-C. & Hirs, C.H.W. (1977) Influence of the heterosaccharides in porcine pancreatic ribonuclease on the conformation and stability of the protein. *J. Biol. Chem.* **252**, 8358–8364.
- Hetch, H.J., Kaliz, H.M., Hendle, J., Schmid, R.D. & Schomburg, D. (1993) Crystal structure of glucose oxidase from *Aspergillus niger* refined at 2.3 Å resolution. *J. Mol. Biol.* **229**, 153–172.
- Dwek, R.A. (1995) Glycobiology: more function for oligosaccharides. *Science* **269**, 1234–1235.
- Masson, P. (1992) Pressure denaturation of proteins. In *High Pressure*

- and Biotechnology* (Balny, C., Hayashi, R., Heremans, K. & Masson, P., eds), Vol. 224, pp. 89–99. John Libbey Eurotext, France.
38. Joao, H.C. & Dwek, R.A. (1993) Effects of glycosylation on protein structure and dynamics in ribonuclease B and some of its individual glycoforms. *Eur. J. Biochem.* **218**, 239–244.
39. Rudd, P.M., Joao, H.C., Coghill, E., Fiten, P., Saunders, M.R., Opedenakker, G. & Dwek, R.A. (1994) Glycoforms modify the dynamic stability and functional activity of an enzyme. *Biochemistry* **33**, 17–22.
40. Tams, J.W. & Welinder, K.G. (1998) Glycosylation and thermodynamic versus kinetic stability of horseradish peroxidase. *FEBS Lett.* **421**, 234–236.